Inorg. Chem. **2006**, *45*, 5561–5567

Spectroscopic Characterization of Primary and Secondary Phosphine Ligation on Ruthenium(II) Complexes

Shadrick I. M. Paris,[†] Jeffrey L. Petersen,[‡] Evamarie Hey-Hawkins,*[,§] and Michael P. Jensen*[,†]

Department of Chemistry and Biochemistry, Ohio University, Athens, Ohio 45701, C. Eugene Bennett Department of Chemistry, West Virginia University, Morgantown, West Virginia 26506, and Fakultät für Chemie und Mineralogie, Institut für Anorganische Chemie, Universität Leipzig, Johannisallee 29, D-04103 Leipzig, Germany

Received November 8, 2005

Ruthenium(II) complexes of the primary phosphines PH_2Fc and PH_2CH_2Fc and the secondary phosphine $PH(CH_2Fc)_2$, including $[(p\text{-cymene})RuCl(L)_2](PF_6)$ (*p*-cymene = *p*-^{i}PrC$_6$H$_4$Me, L = PH_2CH_2Fc and $PH(CH_2Fc)_2$, **2b** and **2c**, respectively) and *trans*-$[RuCl_2(L)_4]$ (L = PH_2Fc, PH_2CH_2Fc, and $PH(CH_2Fc)_2$, **3a**–**c**, respectively) were prepared and characterized by IR, ^{1}H NMR, and ^{31}P NMR spectroscopy. **3b** was additionally characterized by X-ray crystallography. The spectroscopic effects of phosphine ligation were determined. Characteristic downfield shifts of the ^{31}P NMR resonances and increases in energy of the ν(P–H) modes were observed in all cases. Iterative fitting of coupling constants to second-order NMR spectra also resulted in a complete elucidation of ^{31}P–^{1}H and ^{31}P–^{31}P couplings. This analysis provides a basis for considering the influence of coordinate bonding on the observed $^1J_{PH}$ and $^2J_{PP}$ constants.

Introduction

Tertiary organophosphines (PR_3) are ubiquitous as ligands in organometallic coordination chemistry; a wide variety of complexes are known, and some have gained significant technological importance.[1] For example, PPh_3 is used to promote rhodium-catalyzed olefin hydroformylation,[2] palladium phosphine complexes are used for catalytic biaryl couplings,[3] phosphines are used to stabilize ring-opening metathesis polymerization (ROMP) catalyst precursors,[4] and chiral bidentate phosphines are used to access asymmetric catalytic reaction manifolds, such as the stereoselective hydrogenation of prochiral olefins and ketones using homogeneous ruthenium and rhodium catalysts.[5] In contrast, primary (PH_2R) and secondary (PHR_2) phosphines have seen only sparing use as ligands.[1,6] Much of the interest in the resulting complexes lies in their use as synthons for phosphido ($-PR_2$), phosphinidene (=PR), and related complexes, exploiting the lability of the P−H bonds.[7−22] In fact, development of coordination chemistry for primary and

* To whom correspondence should be addressed. E-mail: hey@rz.uni-leipzig.de (E.H.-H.); jensenm@ohio.edu (M.P.J.).
† Ohio University.
‡ West Virginia University.
§ Universität Leipzig.

(1) Downing, J. H.; Smith, M. B. In *Comprehensive Coordination Chemistry II*; McCleverty, J. A., Meyer, T. J., Lever, A. B. P., Eds.; Pergamon: Amsterdam, 2000; Vol. 1, pp 253−296.
(2) Parshall, G. W.; Ittel, S. D. *Homogeneous Catalysis*, 2nd ed.; Wiley: New York, 1992.
(3) Miyaura, N.; Suzuki, A. *Chem. Rev.* **1995**, *95*, 2457−2483.
(4) Dias, E. L.; Nguyen, S. T.; Grubbs, R. H. *J. Am. Chem. Soc.* **1997**, *119*, 3887−3897.
(5) Noyori, R. *Angew. Chem., Int. Ed.* **2002**, *41*, 2008−2022.
(6) Brynda, M. *Coord. Chem. Rev.* **2005**, *249*, 2013−2034.
(7) Bartsch, R.; Heitkamp, S.; Morton, S.; Peters, H.; Stelzer, O. *Inorg. Chem.* **1983**, *22*, 3624−3632.
(8) Esteban, M.; Pequerul, A.; Carmona, D.; Lahoz, F. J.; Martín, A.; Oro, L. A. *J. Organomet. Chem.* **1991**, *402*, 421−434.
(9) Maslennikov, S. V.; Glueck, D. S.; Yap, G. P. A.; Rheingold, A. L. *Organometallics* **1996**, *15*, 2483−2488.
(10) Kourkine, I. V.; Glueck, D. S. *Inorg. Chem.* **1997**, *36*, 5160−5164.
(11) Kourkine, I. V.; Sargent, M. D.; Glueck, D. S. *Organometallics* **1998**, *17*, 125−127.
(12) Torres-Lubián, R.; Rosales-Hoz, M. J.; Arif, A. M.; Ernst, R. D.; Paz-Sandoval, M. A. *J. Organomet. Chem.* **1999**, *585*, 68−82.
(13) Leoni, P.; Marchetti, F.; Papucci, S.; Pasquali, M. *J. Organomet. Chem.* **2000**, *593*−*594*, 12−18.
(14) Termaten, A. T.; Nijbacker, T.; Schakel, M.; Lutz, M.; Spek, A. L.; Lammertsma, K. *Organometallics* **2002**, *21*, 3196−3202.
(15) Termaten, A. T.; Nijbacker, T.; Schakel, M.; Lutz, M.; Spek, A. L.; Lammertsma, K. *Eur. J. Chem.* **2003**, *9*, 2200−2208.
(16) Hey-Hawkins, E.; Kurz, S. *J. Organomet. Chem.* **1994**, *479*, 125−133.
(17) Abdul Hadi, G. A.; Fromm, K.; Blaurock, S.; Jelonek, S.; Hey-Hawkins, E. *Polyhedron* **1997**, *16*, 721−731.
(18) Felsberg, R.; Blaurock, S.; Jelonek, S.; Gelbrich, T.; Kirmse, R.; Voigt, A.; Hey-Hawkins, E. *Chem. Ber./Recueil* **1997**, *130*, 807−812.
(19) Blaurock, S.; Hey-Hawkins, E. *Z. Anorg. Allg. Chem.* **2002**, *628*, 37−40.
(20) Blaurock, S.; Hey-Hawkins, E. *Z. Anorg. Allg. Chem.* **2002**, *628*, 2515−2522.

10.1021/ic0519281 CCC: $33.50
Published on Web 06/09/2006

secondary phosphines has presumably suffered from a reputation for reactivity. However, a number of air-stable primary and secondary phosphines have been reported,[25−27] and an increasing range of metal complexes is also known.[1,6]

Given the general importance of phosphine ligands in coordination chemistry and catalysis, numerous analyses of their donor properties have been described, for example by deriving a comparative steric factor from direct structural information, or electronic properties from indirect spectroscopic effects on ancillary ligands, typically the energies of ν(C≡O) modes of carbonyl coligands.[28] Analogous primary and secondary phosphine complexes alternatively afford a rich array of IR and NMR spectroscopic information directly responsive to the effects of phosphine coordination to a Lewis acidic metal center; the ν(P−H) modes lie in the open 2200−2400 cm^{-1} region of IR spectra, and ^{1}H−^{31}P spin coupling reveals a wealth of information in NMR spectra.[29−39] One can note that primary and secondary phosphine centers retain the possibilities of chelation and chiral modification while offering distinct steric and electronic properties as ligands.

In the present work, we have prepared bis- and tetrakis(phosphine) complexes of the air-stable, solid primary phosphines PH_2Fc[24] and PH_2CH_2Fc[26] (Fc = $C_5H_4FeC_5H_5$, ferrocenyl), as well as the secondary phosphine $PH(CH_2Fc)_2$,[38] at ruthenium(II) centers (Scheme 1), specifically [(*p*-cymene)RuCl(L)$_2$](PF$_6$) (*p*-cymene = *p*-^{i}PrC$_6$H$_4$Me, L = PH_2CH_2Fc and $PH(CH_2Fc)_2$, **2b** and **2c**, respectively) and *trans*-[RuCl$_2$(L)$_4$] (L = PH_2Fc, PH_2CH_2Fc, and $PH(CH_2Fc)_2$, **3a**−**c**, respectively). Monophosphine complexes [(*p*-cymene)RuCl$_2$L] (L = PH_2Fc, PH_2CH_2Fc, and $PH(CH_2Fc)_2$, **1a**−**c**, respectively) were reported previously.[39] Complete IR and NMR spectroscopic analyses have been carried out, which suggest trends in relevant parameters that characterize the coordinate bonding in these complexes.

Scheme 1

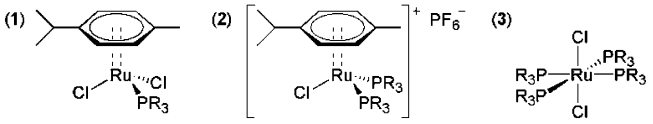

Experimental Section

General Considerations. All manipulations were carried out under inert atmosphere using standard Schlenk techniques.[40] ^{1}H (400 MHz) and ^{31}P (162 MHz) NMR spectra were obtained on a Bruker AVANCE DRX 400 spectrometer and externally referenced to TMS (^{1}H) or 85% H_3PO_4 (^{31}P). Fits to NMR spectra were calculated using the PERCH software package (Perch Solutions, Ltd., Kuopio, Finland). IR spectra were obtained from KBr pellets on a Perkin-Elmer System 2000 spectrophotometer. Elemental analyses were performed by Desert Analytics (Tucson, AZ).

Materials. $RuCl_3 \cdot xH_2O$ was used as received from Merck. [(*p*-cymene)RuCl$_2$]$_2$ and [(*p*-cymene)RuCl(NCMe)$_2$]PF$_6$ were prepared according to literature procedures;[41] α-terpinene (Fluka) was used herein as received from the manufacturer. Preparations of the phosphines PH_2Fc,[24] PH_2CH_2Fc,[26] and $PH(CH_2Fc)_2$[38] were described previously. Reagent grade solvents (acetonitrile, absolute ethanol, hexanes, and anhydrous diethyl ether) were obtained from Aldrich and degassed, dried, and distilled before use by standard techniques. $CDCl_3$ (Cambridge Isotopes) was freshly distilled and degassed prior to use.

[(*p*-cymene)RuCl(PH$_2$CH$_2$Fc)$_2$]PF$_6$ (2b). A 100 mL Schlenk flask was charged with solid samples of [(*p*-cymene)RuCl(NCMe)$_2$]PF$_6$ (100 mg, 0.20 mmol) and PH_2CH_2Fc (103 mg, 0.44 mmol). Acetonitrile (30 mL) was added, and the resulting orange solution was stirred overnight at room temperature. Solvent was then removed under vacuum, affording an orange oil. This oil was triturated with anhydrous diethyl ether (30 mL) overnight, giving a powdery orange solid. The product was washed with anhydrous ether (4 × 30 mL) and dried in vacuo to constant mass (140 mg, 80%). ^{1}H NMR (δ; $CDCl_3$, 25 °C): 1.16 (6H, d, J = 7 Hz, −CH(C*H*$_3$)$_2$); 1.98 (3H, s, -*p*-C*H*$_3$); 2.51 (1H, septet, J = 7 Hz, −C*H*(CH$_3$)$_2$); 3.14 (2H, dddd, $^{2}J_{HH}$ = 14 Hz, $^{3}J_{HH}$ = 7 Hz, 2 Hz, $^{2}J_{PH}$ = 8 Hz, PH$_2$C*H*$_2$Fc); 3.29 (2H, dddd, $^{2}J_{HH}$ = 14 Hz, $^{3}J_{HH}$ = 7 Hz, 7 Hz, $^{2}J_{PH}$ = 7 Hz, PH$_2$C*H*$_2$Fc); 4.19 (10H, s, C$_5$*H*$_5$); 4.22 (4H, br s, C$_5$*H*$_4$); 4.31 (4H, br s, C$_5$*H*$_4$); 4.45 (2H, m, P*H*$_2$CH$_2$Fc); 4.87 (2H, m, P*H*$_2$CH$_2$Fc); 5.52 (2H, d, J = 6 Hz, C$_6$*H*$_4$); 5.74 (2H, d, J = 6 Hz, C$_6$*H*$_4$). ^{31}P{^{1}H} (δ; $CDCl_3$, 25 °C): −24.9 (s, *P*H$_2$CH$_2$Fc); −144.1 (septet, $^{1}J_{PF}$ = 714 Hz, *P*F$_6^-$). LSI-MS: m/z = 735.0 ([M]$^+$), 502.9 ([M − PH$_2$CH$_2$Fc]$^+$) [100], 466.9 ([M − PH$_2$CH$_2$Fc − HCl]$^+$) [56], 347.0 ([M − PH$_2$CH$_2$Fc − Cl − Fe(C$_5$H$_5$)]$^+$) [31]. Anal. Calcd (Found) for $C_{32}H_{40}ClF_6Fe_2P_3Ru$: C, 43.68 (43.46); H, 4.59 (4.56).

[(*p*-cymene)RuCl{PH(CH$_2$Fc)$_2$}$_2$]PF$_6$ (2c). The complex was prepared from [(*p*-cymene)RuCl(NCMe)$_2$]PF$_6$ (100 mg, 0.20 mmol) and $PH(CH_2Fc)_2$ (190 mg, 0.44 mmol) as described for **2b** above, yielding a solid orange product (240 mg, 94% yield). ^{1}H NMR (δ;

(21) Blaurock, S.; Hey-Hawkins, E. *Eur. J. Inorg. Chem.* **2002**, 2975−2984.
(22) Felsberg, R.; Blaurock, S.; Junk, P. C.; Kirmse, R.; Voigt, A.; Hey-Hawkins, E. *Z. Anorg. Allg. Chem.* **2004,** *630*, 806−816.
(23) Bartlett, R. A.; Olmstead, M. M.; Power, P. P.; Sigel, G. A. *Inorg. Chem.* **1987**, *26*, 1941−1946.
(24) Spang, C.; Edelmann, F. T.; Noltemeyer, M.; Roesky, H. W. *Chem. Ber.* **1989**, *122*, 1247−1254.
(25) Prabhu, K. R.; Pillarsetty, N.; Gali, H.; Katti, K. V. *J. Am. Chem. Soc.* **2000**, *122*, 1554−1555.
(26) Goodwin, N. J.; Henderson, W.; Nicholson, B. K.; Fawcett, J.; Russell, D. R. *J. Chem. Soc., Dalton Trans.* **1999**, 1785−1793.
(27) Henderson, W.; Alley, S. R. *J. Organomet. Chem.* **2002**, *656*, 120−128.
(28) Tolman, C. A. *Chem. Rev.* **1977**, *77*, 313−348.
(29) Palmer, R. A.; Whitcomb, D. R. *J. Magn. Reson.* **1980**, *39*, 371−379.
(30) Dyson, D. B.; Parish, R. V.; McAuliffe, C. A.; Pritchard, R. G.; Fields, R.; Beagley, B. *J. Chem. Soc., Dalton Trans.* **1989**, 907−914.
(31) Leoni, P. *Organometallics* **1993**, *12*, 2432−2434.
(32) Kourkine, I. V.; Maslennikov, S. V.; Ditchfield, R.; Glueck, D. S.; Yap, G. P. A.; Liable-Sands, L. M.; Rheingold, A. L. *Inorg. Chem.* **1996**, *35*, 6708−6716.
(33) Giannandrea, R.; Mastrorilli, P.; Palma, M.; Fanizzi, F. P.; Englert, U.; Nobile, C. F. *Eur. J. Inorg. Chem.* **2000**, 2573−2576.
(34) Pelczar, E. M.; Nytko, E. A.; Zhuravel, M. A.; Smith, J. M.; Glueck, D. S.; Sommer, R.; Incarvito, C. D.; Rheingold, A. L. *Polyhedron* **2002**, *21*, 2409−2419.
(35) Stulz, E.; Maue, M.; Scott, S. M.; Mann, B. E.; Sanders, J. K. M. *New J. Chem.* **2004**, *28*, 1066−1072.
(36) Xie, J.; Huang, J.-S.; Zhu, N.; Zhou, Z.-Y.; Che, C.-M. *Eur. J. Chem.* **2005**, *11*, 2405−2416.
(37) Sommer, R.; Lönnecke, P.; Baker, P. K.; Hey-Hawkins, E. *Inorg. Chem. Commun.* **2002**, *5*, 115−118.
(38) Sommer, R.; Lönnecke, P.; Reinhold: J.; Baker, P. K.; Hey-Hawkins, E. *Organometallics* **2005**, *24*, 5256−5266.
(39) Paris, S. I. M.; Lemke, F. R.; Sommer, R.; Lönnecke, P.; Hey-Hawkins, E. *J. Organomet. Chem.* **2005**, *690*, 1807−1813.
(40) Shriver, D. F.; Drezdzon, M. A. *Manipulation of Air-Sensitive Compounds*, 2nd ed.; Wiley-Interscience: New York, 1986.
(41) Jensen, S. B.; Rodger, S. J.; Spicer, M. D. *J. Organomet. Chem.* **1998**, *556*, 151−158.

$CDCl_3$, 25 °C): 1.22 (6H, d, $J = 7$ Hz, $-CH(CH_3)_2$); 1.89 (3H, s, $-CH_3$); 2.51 (1H, sep, $J = 7$ Hz, $-CH(CH_3)_2$); 2.77 (2H, ddd, $^2J_{HH} = 15$ Hz, $^3J_{HH} = 8$ Hz, $^2J_{PH} = 5$ Hz, $PH(CH_2Fc)_2$); 2.96 (4H, m, $PH(CH_2Fc)_2$); 3.30 (2H, ddd, $^2J_{HH} = 15$ Hz, $^3J_{HH} = 4$ Hz, $^2J_{PH} = 11$ Hz, $PH(CH_2Fc)_2$); 4.02 (2H, m, $PH(CH_2Fc)_2$); 4.13 (10H, s, C_5H_5); 4.15 (10H, s, C_5H_5); 4.18 (16H, br m, C_5H_4); 5.58 (2H, d, $J = 6$ Hz, C_6H_4); 5.64 (2H, d, $J = 6$ Hz, C_6H_4). $^{31}P\{^1H\}$ NMR (δ; $CDCl_3$, 25 °C): 31.8 (s, $PH_2(CH_2Fc)_2$); −144.0 (septet, $^1J_{PF} = 714$ Hz, PF_6^-). LSI-MS: $m/z = 1131.1$ ($[M]^+$), 701.1 ($[M - PH(CH_2Fc)_2]^+$) [100], 665.1 ($[M - PH(CH_2Fc)_2 - HCl]^+$) [64]. Anal. Calcd (Found) for $C_{54}H_{60}ClF_6Fe_4P_3Ru$: C, 50.83 (50.21); H, 4.75 (4.69).

***trans*-[RuCl$_2$(PH$_2$Fc)$_4$] (3a).** A 100 mL Schlenk flask was charged with $RuCl_3$ (50 mg, 0.24 mmol) and PH_2Fc (265 mg, 1.21 mmol). Absolute ethanol (50 mL) was added, and the resulting green solution was refluxed for 2 h, resulting in a yellow suspension. Volatiles were removed under vacuum, affording an ochre-yellow solid. The product was washed with hexanes (3×40 mL) and dried under vacuum to constant weight (90 mg, 36% yield). ^1H NMR (δ; $CDCl_3$, 25 °C): 4.11 (20H, s, C_5H_5); 4.32 (8H, br s, C_5H_4); 4.42 (8H, br s, C_5H_4); 5.36 (8H, m, PH_2Fc). $^{31}P\{^1H\}$ NMR (δ; $CDCl_3$, 25 °C): −27.2. LSI-MS: $m/z = 1043.8$ ($[M]^+$) with fragmentation. Anal. Calcd (Found) for $C_{40}H_{44}Cl_2Fe_4P_4Ru$: C, 46.01 (46.02); H, 4.26 (4.45).

***trans*-[RuCl$_2$(PH$_2$CH$_2$Fc)$_4$] (3b).** The complex was prepared from $RuCl_3$ (50 mg, 0.24 mmol) and PH_2CH_2Fc (280 mg, 1.21 mmol) as described for **3a**. An ochre-yellow product was obtained (170 mg, 64% yield). ^1H NMR (δ; $CDCl_3$, 25 °C): 2.94 (8H, dt, $^3J_{HH} = 7$ Hz, PH_2CH_2Fc); 4.14 (20H s, C_5H_5); 4.16 (8H, br s, C_5H_4); 4.22 (8H, br s, C_5H_4); 4.55 (8H, m, PH_2CH_2Fc). $^{31}P\{^1H\}$ NMR (δ; $CDCl_3$, 25 °C): −20.7. LSI-MS: $m/z = 1099.9$ ($[M]^+$) with fragmentation. Anal. Calcd (Found) for $C_{44}H_{52}Cl_2Fe_4P_4Ru$: C, 48.03 (48.06); H, 4.77 (4.84).

***trans*-[RuCl$_2${PH(CH$_2$Fc)$_2$}$_4$] (3c).** The complex was prepared from $RuCl_3$ (50 mg, 0.24 mmol) and $PH(CH_2Fc)_2$ (518 mg, 1.21 mmol) as described for **3a**, yielding a green product (280 mg, 61% yield). ^1H NMR (δ; $CDCl_3$, 25 °C): 2.47 (8H, ddd, $^2J_{PH} < 2$ Hz, $^2J_{HH} = 14$ Hz, $^3J_{HH} = 6$ Hz, $PH(CH_2Fc)_2$); 3.24 (8H, ddd, $^2J_{PH} < 2$ Hz, $^2J_{HH} = 14$ Hz, $^3J_{HH} = 3$ Hz, $PH(CH_2Fc)_2$); 3.90 (16H, br s, C_5H_4); 4.09 (40H, s, C_5H_5); 4.21 (16H, br s, C_5H_4); the P*H* signal was not distinguishable. $^{31}P\{^1H\}$ NMR (δ; $CDCl_3$, 25 °C): 30.6. LSI-MS: $m/z = 1892.0$ ($[M]^+$) with fragmentation. Anal. Calcd (Found) for $C_{88}H_{92}Cl_2Fe_8P_4Ru$: C, 55.86 (54.50); H, 4.90 (4.91).

X-ray Structure Determination of *trans*-[RuCl$_2$(PH$_2$CH$_2$Fc)$_4$] (3b). X-ray quality crystals of **3b** were grown by slow evaporation of a CH_2Cl_2 solution, giving yellow plates. A single crystal was washed with perfluoropolyether PFO-XR75 (Lancaster) and sealed in a glass capillary. The sample was optically aligned on the four-circle of a Siemens P4 diffractometer equipped with a Mo Kα radiation source ($\lambda = 0.71031$ Å), graphite monochromatic crystal, and a SMART CCD detector. Data were collected at room temperature. Four sets of 20 frames each were collected using the ω scan method with a 10 s exposure time. Integration of these frames followed by reflection indexing and least squares refinement produced a crystal orientation matrix and preliminary lattice parameters for the monoclinic cell. The program SMART (version 5.6) was used for diffractometer control, frame scans, indexing, orientation matrix calculations, least squares refinement of cell parameters, and the data collection. A total of 1650 frames were collected with 30 s exposures in five different runs covering a hemisphere of data. All raw data frames were read by the program SAINT (version 5/6.0) and integrated using 3D profiling algorithms. An absorption correction was applied using the SADABS routine available in SAINT. The data were corrected for Lorentz and polarization effects. The structure was solved by a combination of direct methods and Fourier methods using SHELXTL 6.1. The ruthenium atom lies on a crystallographic center of inversion symmetry. Idealized hydrogen atom positions were included as fixed contributions using a riding model with isotropic temperature factors set at 1.2 times that of the adjacent carbon. A summary of the refinement is given in Table 1. An ORTEP representation of the refined structure is shown in Figure 1 (relevant bond lengths and angles are summarized in the caption).

Table 1. Summary of the X-ray Data Collection for **3b**

formula	$C_{44}H_{52}Cl_2Fe_4P_4Ru$
fw	1100.11
T, K	295(2)
space group	monoclinic, $P2_1/c$
a, Å	14.842(2)
b, Å	11.484(2)
c, Å	12.843(2)
β	103.490(2)
V, Å^3	2128.7(5)
Z	2
ρ_{calc}, g/cm^3	1.716
total reflns	14 792
independent reflns	4825
params	250
R1 (%)[a]	5.54
wR2 (%)[a]	8.72

[a] All data.

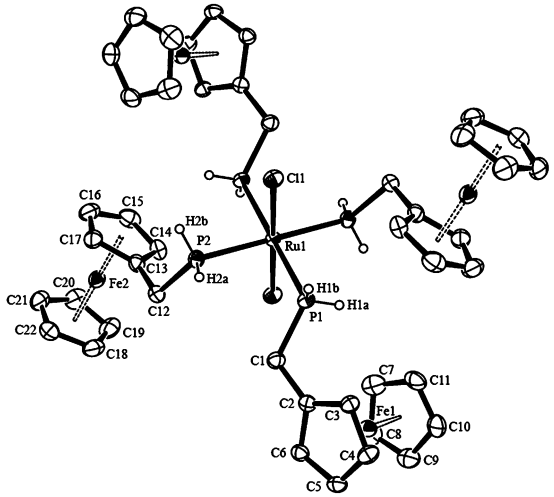

Figure 1. ORTEP drawing of *trans*-[$RuCl_2(PH_2CH_2Fc)_4$] (**3b**), with ellipsoids displayed at 30% probability. Carbon-bonded hydrogen atoms are omitted for clarity. Selected bond distances (Å): Ru−Cl1, 2.4397(7); Ru−P1, 2.3127(8); Ru−P2, 2.3129(8); P1−C1, 1.834(3); C1−C2, 1.493(4); P2−C12, 1.843(3); C12−C13, 1.492(4). Selected bond angles (deg): P1−Ru−P2, 90.09(3); P1−Ru−P2′, 89.91(3); P1−Ru−Cl1, 93.35(3); P1−Ru−Cl1′, 86.65(3); P2−Ru−Cl1, 85.61(3); P2−Ru−Cl1′, 94.39(3); Ru−P1−C1, 119.2(1); P1−C1−C2, 115.8(2); Ru−P2−C12, 121.4(1); P2−C12−C13, 110.7(2).

Results

We have utilized a range of air-stable ferrocenyl-substituted primary and secondary phosphines in order to obtain robust ruthenium(II) complexes. Preparation and characterization of monophosphine complexes of the formula [(*p*-cymene)$RuCl_2(PR_3)$] ($PR_3 = PH_2Fc$ (**1a**), PH_2CH_2Fc (**1b**), $PH(CH_2Fc)_2$ (**1c**), Scheme 1) were described previously.[39] In the present work, we have prepared bis(phosphine) complex salts of formula [(*p*-cymene)$RuCl(PR_3)_2$]PF_6

Table 2. Selected NMR and IR Parameters for Phosphines and the Ruthenium(II) Complexes[a]

complexes	ν(P−H) (cm^{-1})	δ_H (ppm)	δ_P (ppm)	$^1J_{PH}$ (Hz)	ref
[(*p*-cymene)RuCl$_2$(PH$_2$Fc)] (**1a**)	2340	5.69	−27.6	394	39
[(*p*-cymene)RuCl$_2$(PH$_2$CH$_2$Fc)] (**1b**)	2338	4.82	−27.7	359	39
[(*p*-cymene)RuCl$_2${PH(CH$_2$Fc)$_2$}] (**1c**)	2375	4.72	24.7	351	39
[(*p*-cymene)RuCl(PH$_2$CH$_2$Fc)$_2$]PF$_6$ (**2b**)	2346	4.45, 4.87	−24.9	373, 370	*c*
[(*p*-cymene)RuCl{PH(CH$_2$Fc)$_2$}$_2$]PF$_6$ (**2c**)	2343	4.02	31.8	366	*c*
trans-[RuCl$_2$(PH$_2$Fc)$_4$] (**3a**)	2327	5.35	−27.2	347	*c*
trans-[RuCl$_2$(PH$_2$CH$_2$Fc)$_4$] (**3b**)	2326	4.54	−20.7	330	*c*
trans-[RuCl$_2${PH(CH$_2$Fc)$_2$}$_4$] (**3c**)	2312	*b*	30.6	332	*c*
PH$_2$Fc	2259	3.82	−143.3	203	24
PH$_2$CH$_2$Fc	2285	2.94	−129.1	194	26
PH(CH$_2$Fc)$_2$	2285	3.31	−53.4	196	38

[a] ^{31}P NMR data recorded in CDCl$_3$ at 25 °C; IR data recorded from KBr pellets. [b] The peaks were not directly observed. [c] This work.

Scheme 2

$$[(p\text{-cymene})RuCl_2]_2 + 2.2NH_4PF_6 \xrightarrow[25\ °C,\ 16\ h]{NCMe} 2[(p\text{-cymene})RuCl(NCMe)_2]PF_6$$

$$[(p\text{-cymene})RuCl(NCMe)_2]PF_6 + 2.2PR_3 \xrightarrow[25\ °C,\ 16\ h]{NCMe} [(p\text{-cymene})RuCl(PR_3)_2]PF_6\ (\mathbf{2})$$

$$PR_3 = PH_2CH_2Fc\ (\mathbf{b}),\ PH(CH_2Fc)_2\ (\mathbf{c})$$

Scheme 3

$$RuCl_3 + xsPR_3 \xrightarrow[reflux,\ 2\ h]{EtOH\ (abs.)} trans\text{-}[RuCl_2(PR_3)_4]\ (\mathbf{3})$$

$$PR_3 = PH_2Fc\ (\mathbf{a}),\ PH_2CH_2Fc\ (\mathbf{b}),\ PH(CH_2Fc)_2\ (\mathbf{c})$$

(PR$_3$ = PH$_2$CH$_2$Fc (**2b**), PH(CH$_2$Fc)$_2$ (**2c**)) by simple ligand substitution of the complex [(*p*-cymene)RuCl(NCMe)$_2$]PF$_6$ (Scheme 2);[41] attempted preparation of the PH$_2$Fc analogue **2a** generated multiple phosphorus-containing species, as shown by ^{31}P NMR. We also prepared the tetrakis(phosphine) complexes of general formula *trans*-[RuCl$_2$(PR$_3$)$_4$] (PR$_3$ = PH$_2$Fc (**3a**), PH$_2$CH$_2$Fc (**3b**), PH(CH$_2$Fc)$_2$ (**3c**)) from the previously demonstrated in situ reduction of RuCl$_3$·*x*H$_2$O in the presence of excess phosphines in EtOH solution (Scheme 3).[42−45] The products were fully characterized by IR spectroscopy, ^{1}H and ^{31}P NMR spectroscopy, mass spectrometry, and elemental analysis, although in the latter case, carbon analyses of both **2c** and **3c** were slightly low. The solid materials were air and water stable but displayed mild sensitivity in solution.

The tetrakis(phosphine) complex **3b** was further characterized by X-ray crystallography (Figure 1). The observed octahedral structure is similar to previously characterized PHMe$_2$,[43] PHPh$_2$,[44] PH$_2$Ph,[45] and related analogues;[46] the Ru−P bond lengths of 2.3127(8) and 2.3129(8) Å and the Ru−Cl bond length of 2.4397(7) Å lie within the narrow range observed for the analogues, 2.318(3)−2.367(1) and 2.422(3)−2.450(1) Å, respectively. The Ru−P and Ru−Cl coordinate bond lengths are also comparable to those of **1c**.[39] The complex is slightly distorted from ideal D_{4h} symmetry, exhibiting a tilt of the rigorously linear Cl−Ru−Cl vector with respect to the P$_4$Ru equatorial plane. This distortion was also observed, to a lesser extent, in related complexes.[45] A unique aspect of this structure is the four ferrocenylmethyl substituents on the phosphines, which are clearly disposed to minimize intramolecular steric contact. In keeping with the inversion symmetry, two of these substituents lie above the ruthenium−phosphorus plane and two below, with each pair further oriented in a staggered arrangement. The non-hydrogen atom geometry of each ligand is identical to that of the free phosphine, except for an extremely slight contraction of the phosphorus−carbon bond lengths from a distance of 1.850(3) Å.[26] The Ru−P−CH$_2$R angles of ca. 120° are also typical.[39,43−46]

Complexes **2b,c** and **3a−c** displayed singlet ^{31}P{^{1}H} NMR spectra arising from the chemically equivalent ligated phosphines, as well as a septuplet peak arising from the (PF$_6$)$^-$ counterion for **2b,c**. ^{1}H NMR spectra were also consistent with the assigned complex structure (vide supra). The expected downfield shifts of resonances for the bound ligands versus free phosphines were observed in all cases (Table 2). An increase in energy of the ν(P−H) mode characteristic of ligation was also observed by IR spectroscopy. Similar spectroscopic results have been reported for **1a−c** and related complexes. [39]

In the case of complexes **1a−c**, increased $^1J(^1H-^{31}P)$ values were also directly diagnostic of ligand coordination. However, evaluation of this parameter for **2b,c** and **3a−c** was complicated by magnetic inequivalence in the ^{1}H and ^{1}H-coupled ^{31}P NMR spectra, which give rise to second-order multiplicity arising from $^2J(^{31}P-^{31}P)$ coupling. Considering the wealth of spectroscopic information contained within these data, iterative computer simulations of the ^{1}H-coupled ^{31}P NMR were performed to extract approximate values of the various coupling constants. In the single case

(42) Sanders, J. R. *J. Chem. Soc. A*, **1971**, 2991−2995.
(43) Cotton, F. A.; Frenz, B. A.; Hunter, D. L. *Inorg. Chim. Acta* **1976**, *16*, 203−207.
(44) McAslan, E. B.; Blake, A. J.; Stephenson, T. A. *Acta Crystallogr. C* **1989**, *45*, 1811−1813.
(45) Blake, A. J.; Champness, N. R.; Forder, R. J.; Frampton, C. S.; Frost, C. A.; Reid, G.; Simpson, R. H. *J. Chem. Soc., Dalton Trans*. **1994**, 3377−3382.
(46) Higham, L.; Powell, A. K.; Whittlesey, M. K.; Wocadlo, S.; Wood, P. T. *J. Chem. Soc., Chem. Commun.* **1998**, 1107−1108.

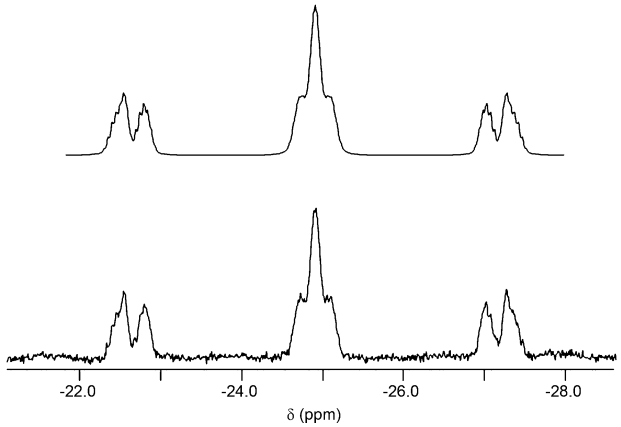

Figure 2. Experimental (bottom) and simulated (top) ^{1}H-coupled ^{31}P NMR spectra of the primary phosphine complex [(*p*-cymene)RuCl($PH_2CH_2Fc)_2$]-PF_6 (**2b**) in $CDCl_3$.

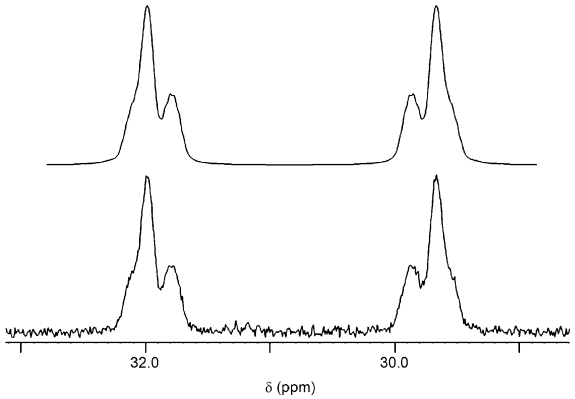

Figure 3. Experimental (bottom) and simulated (top) ^{1}H-coupled ^{31}P NMR spectra of the secondary phosphine complex [(*p*-cymene)RuCl{$PH(CH_2Fc)_2\}_2$]PF_6 (**2c**) in $CDCl_3$.

of complex **3a**, the second-order PH_2Fc ^{1}H resonance was fully resolved and was simulated as well, with concordant results.

Complexes **2b,c** display complex coupling patterns arising from $[AWXYZ]_2$ and $[AVWXYZ]_2$ spin systems, respectively, in which the large number of distinct spins are due to the diastereotopic protons on the phosphorus and/or methylene carbons. Notwithstanding this complexity, the spin physics of simple $X_nAA'X'_n$ spin systems are relevant to these systems,[47−49] owing to the relatively large $^1J_{PH}$ and $^2J_{PP}$ couplings; approximate first-order patterns are still observed for **2b,c**, reflecting the large one-bond ^{1}H−^{31}P coupling. The experimental ^{1}H-coupled ^{31}P NMR resonances and simulations are shown (Figures 2 and 3); the spectrum of **2b** is an approximate triplet, $^1J_{PH}$ = 373, 369 Hz, while that of **2c** resembles a doublet, $^1J_{PH}$ = 366 Hz. The fitted values closely approach those directly observed for the monophosphine complexes **1a**−**c** in rigorously first-order spectra (Table 2) and again are significantly larger than those of the free phosphines. The second-order complexity derives from two-bond ^{31}P−^{31}P coupling, $^2J_{PP}$ = 56 Hz for **2b**, and $^2J_{PP}$ = 50 Hz for **2c** (note that the absolute signs of $^2J_{PP}$ are not

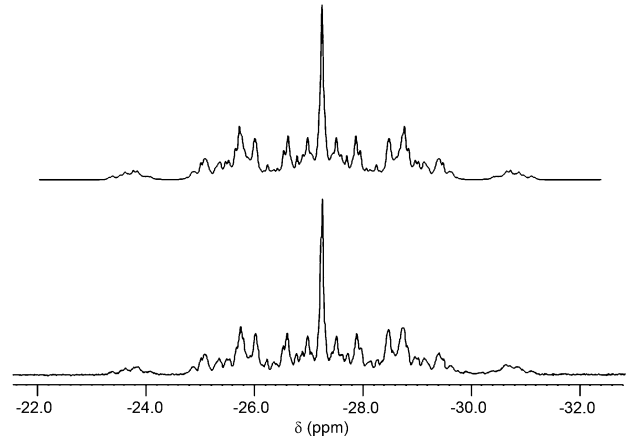

Figure 4. Experimental (bottom) and simulated (top) ^{1}H-coupled ^{31}P NMR spectra of the primary phosphine complex *trans*-[$RuCl_2(PH_2Fc)_4$] (**3a**) in $CDCl_3$.

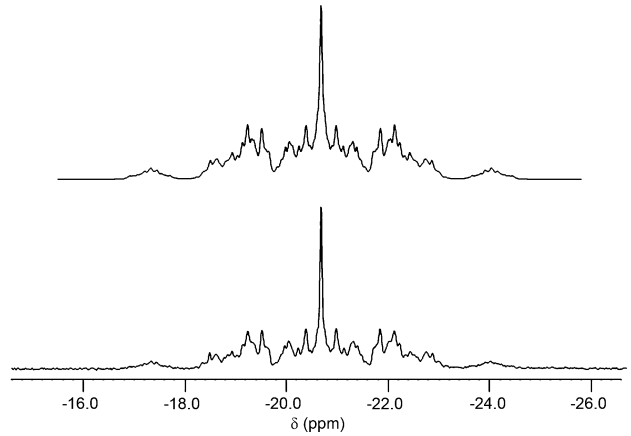

Figure 5. Experimental (bottom) and simulated (top) ^{1}H-coupled ^{31}P NMR spectra of the primary phosphine complex *trans*-[$RuCl_2(PH_2CH_2Fc)_4$] (**3b**) in $CDCl_3$.

determined for **2b,c**). The smaller remaining coupling constants obtained for complex **2b** were $^2J_{PH}$ = 8, 7 Hz, $^3J_{PH}$ = 13, 3 Hz. The values obtained for complex **2c** were quite similar: $^2J_{PH}$ = 12, 8, 6, and 5 Hz, $^3J_{PH}$ = 8 Hz.

The ^{1}H-coupled ^{31}P NMR spectra of the tetrakis(phosphine) complexes **3a**−**c** are more complex than those obtained for complexes **2a,b** (Figures 4−6). The trans geometries give rise to significantly larger $^2J_{PP}$ values, evident in the much wider signal dispersions. The spectrum of the secondary phosphine complex **3c** still features obvious doublet lines arising from ^{1}H−^{31}P coupling, but the triplet patterns of the primary PH_2Fc and PH_2CH_2Fc phosphine complexes, **3a** and **3b**, respectively, are much harder to discern (see commentary in Supporting Information). Comparison of the latter spectra indicates that the methylene proton couplings are largely unresolved. Therefore, simulations were simplified by fitting an $[AX_2]_4$ spin system for the primary phosphine complexes **3a** and **3b**, and $[AX]_4$ for the secondary phosphine analogue **3c**. The simulated spectra obtained for **3a**−**c** closely correspond to the observed data (Figures 4−6). The coupling constants are as follows. **3a**, $^1J_{PH}$ = 347 Hz, $^2J_{PPtrans}$ = 342 Hz, $^2J_{PPcis}$ = −38 Hz, $^3J_{PHtrans}$ = 0 Hz, $^3J_{PHcis}$ = 8 Hz; **3b**, $^1J_{PH}$ = 330 Hz, $^2J_{PPtrans}$ = 328 Hz, $^2J_{PPcis}$ = −40 Hz, $^3J_{PHtrans}$ = 0 Hz,

(47) Harris, R. K. *Can. J. Chem.* **1964**, *42*, 2275−2281.
(48) Mowthorpe, D. J.; Chapman, A. C. *Spectrochim. Acta* **1967**, *23A*, 451−453.
(49) Mann, B. E. *J. Chem. Soc. A* **1970**, 3050−3053.

Table 3. $^1J_{PH}$ and $^2J_{PP}$ (trans and cis) for a Series of Bis- and Tetrakis(phosphine) Complexes

complexes	$^1J_{PH}$ (Hz)	$^2J_{PP}$ (Hz) (trans)	$^2J_{PP}$ (Hz) (cis)[b]	ref
[(*p*-cymene)RuCl($PH_2CH_2Fc)_2$]PF_6 (**2b**)	373, 370	−	56	*a*
[(*p*-cymene)RuCl{$PH(CH_2Fc)_2\}_2$]PF_6 (**2c**)	366	−	50	*a*
trans-[$RuCl_2(PH_2Fc)_4$] (**3a**)	347	342	−38	*a*
trans-[$RuCl_2(PH_2CH_2Fc)_4$] (**3b**)	330	328	−40	*a*
trans-[$RuCl_2\{PH(CH_2Fc)_2\}_4$] (**3c**)	332	300	−39	*a*
[$Pd(PH^tBu_2)_3$]	256	−	−	31
[$Ni(PH_2Mes)_4$]	283	−	33[c]	32
[$Cu(PH_2Mes)_4$][PF_6]	317	−	−	32
[$Pd(PH_2Mes)_4$][BF_4]$_2$	422	394	−30	32
[Ru(por)$\{PH_2(PA)\}_2$][d]	341	621	−	35
[$Ru(F_{20}$-tpp)$(PH_2Ph)_2$][e]	330	510	−	36
[Ru(4-MeO-tpp)$(PHPh_2)_2$][f]	338	500	−	36
[$CpRu(PPh_3)(PHPh_2)Cl$][g]	360	−	47	57
[$Cp^*Ru(PPh_3)(PHPh_2)Cl$][h]	362	−	43	57

[a] This work. [b] Sign undetermined unless specified. [c] Tetrahedral. [d] por = 5,10-bis(3,5-di-*tert*-butylphenyl)-2,8,12,18-tetraethyl-3,7,13,17-tetramethylporphyrindiato; PA = phenylacetylene phosphine. [e] F_{20}-tpp = 5,10,15,20-tetrakis(pentafluorophenyl)porphyrindiato. [f] 4-MeO-tpp = 5,10,15,20-tetrakis(4-methoxyphenyl)porphyrindiato. [g] Cp = η^5-C_5H_5. [h] Cp* = η^5-C_5Me_5.

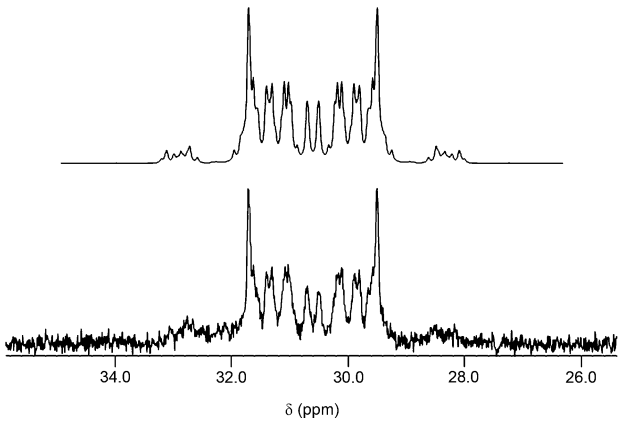

Figure 6. Experimental (bottom) and simulated (top) ^{1}H-coupled ^{31}P NMR spectra of the secondary phosphine complex *trans*-[$RuCl_2\{PH(CH_2Fc)_2\}_4$] (**3c**) in $CDCl_3$.

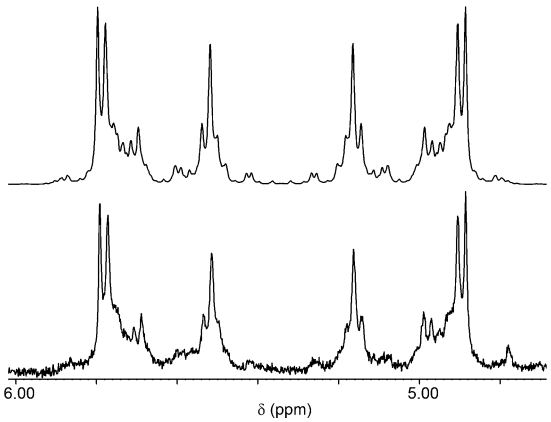

Figure 7. Experimental (bottom) and simulated (top) PH_2Fc proton resonances from the ^{1}H NMR spectrum of *trans*-[$RuCl_2(PH_2Fc)_4$] (**3a**) in $CDCl_3$.

$^3J_{PHcis}$ = 12 Hz; **3c**, $^1J_{PH}$ = 332 Hz, $^2J_{PPtrans}$ = 300 Hz, $^2J_{PPcis}$ = −39 Hz, $^3J_{PHtrans}$ = 0 Hz, $^3J_{PHcis}$ = 14 Hz (only the relative signs of $^2J_{PPtrans}$ and $^2J_{PPcis}$ are determined by simulation, and we take $^2J_{PPtrans} > 0$, $^2J_{PPcis} < 0$ for **3a**−**c** by literature precedent). Inclusion of coupling from the methylene protons, less than 5 Hz, merely served to broaden the simulated peaks.

Observation of an unobstructed ^{1}H NMR signal for the PH_2Fc protons of **3a** allowed us to independently confirm the results of the simulation to the ^{1}H-coupled ^{31}P NMR data (Figure 7). A slightly higher first-order splitting was indicated by the ^{1}H NMR simulation, $^1J_{PH}$ = 368 Hz, but the other parameters were identical, $^2J_{PPtrans}$ = 342 Hz, $^2J_{PPcis}$ = −38 Hz, $^3J_{PHtrans}$ = 0 Hz, $^3J_{PHcis}$ = 8 Hz. The slight discrepancy probably results from the weak, broad outer lines in the ^{31}P data ($\Delta\delta$ = 0.06 ppm), and provides a useful independent estimate of the accuracy of the $^1J_{PH}$ values obtained from the iterative fitting of such data.

Discussion

The IR and NMR spectroscopic data of complexes **2b,c** and **3a**−**c** exhibit several parameters that can be associated with primary and secondary phosphine coordination (Tables 2 and 3). First, there is a significant increase in the magnitude of $^1J_{PH}$ for ruthenium(II)-bound phosphine complexes compared the free phosphines (Table 2). This effect is postulated to result from enhanced s-orbital character in the P−H bond(s) of the coordinated phosphine (Bent's rules),[50] consistent with a rehybridization toward sp^2;[43] this increases the Fermi contact, adding a large, positive contribution to the observed coupling. Thus, one has the range of $^1J_{PH}$ values: [$Pd(PH^tBu_2)_3$], 256 Hz;[31] [$Ni(PH_2Mes)_4$], 283 Hz;[32] [$Cu(PH_2Mes)_4$]$^+$, 317 Hz;[32] *trans*-[$RuCl_2(L)_4$] (**3a**−**c**), 330−347 Hz; [$Pd(PH_2Mes)_4$]$^{2+}$, 422 Hz (Table 3).[32] These data seem generally consistent with the proposal that the increase in $^1J_{PH}$ approximately correlates with the Lewis acidity of the complexed metal ion and hence with the σ-donor strength of the phosphine.[6,32]

A potentially related spectroscopic parameter is the energy of the ν(P−H) mode(s) observed by IR spectroscopy. This stretching shifts to higher energy relative to the free phosphine for all the ruthenium(II) complexes **1a**−**c**, **2b,c**, and **3a**−**c**, consistent with P−H bond strengthening on ligation (Table 2). However, this effect must be a composite of various factors in addition to rehybridization and is absent or even reversed in other transition metal complexes.[32]

(50) Bent, H. A. *Chem. Rev.* **1961**, *61*, 275−311.

Within these available data, there appears to be no particular correlation between $^1J_{PH}$ and ν(P−H).

The bis- and tetrakis(phosphine) complexes **2b,c** and **3a**−**c** exhibit second-order ^{31}P NMR spectra in the presence of ^{31}P−^{1}H coupling due to magnetic inequivalence resulting from the condition $^1J_{PH} \neq {}^3J_{PH}$. This leads to observable $^2J_{PP}$ coupling, and the values of the coupling constants can be determined by iterative simulation (Tables 2 and 3 and Supporting Information). The $^2J_{PP}$ coupling constants display the expected geometry dependence with respect to both magnitude and sign on comparison of the cis and trans values obtained, $^2J_{PPtrans} > {}^2J_{PPcis}$ with opposite relative signs; this dependence has been well documented in octahedral and square-planar complexes of tertiary organophosphines, with the general rule being $^2J_{PPtrans} > {}^2J_{PPcis}$ for such systems.[51−56] Moreover, the primary phosphine complexes **3a,b** exhibit ^{1}H-coupled ^{31}P spectra that are quite similar to that of the square-planar complex $[Pd(PH_2Mes)_4]^{2+}$, which yields similar cis and trans $^2J_{PP}$ values with respect to both magnitude and sign (Table 3).[32] Additionally, the tetrahedral compound $[Ni(PH_2Mes)_4]$ exhibits a $^2J_{PP}$ value on par with that of the cis couplings in **2b,c** and **3a**−**c**.[32] Also noteworthy are the first-order couplings between chemically inequivalent ^{31}P nuclei with an absolute magnitude of 37−47 Hz in the complexes $[CpRu(PPh_3)(PHPh_2)Cl]$ (Cp = C_5H_5),[57] $[Cp^*Ru(PPh_3)(PHPh_2)Cl]$ (Cp* = C_5Me_5),[57] and *trans,trans,trans*-$[RuCl_2\{P(CH_2OH)_3\}_2\{P(CH_2OH)_2H\}_2]$.[56]

Apart from the obvious geometric effects, coordinate bonding and phosphorus rehybridization should also exert an influence on $^2J_{PP}$ magnitudes. For example, correlation of $^2J_{PP}$ to phosphine ligand basicity was observed in first-order spectra of mixed-ligand complexes $[Fe(CO)_3(L)(L')]$.[58] Compared to the domination of $^1J_{PH}$ coupling by the Fermi contact term, interpretation of any such trend in $^2J_{PP}$ is complicated by other contributions. For example, geometrically equivalent trans couplings in three complexes of various primary phosphines at ruthenium(II) porphyrins range from 500 to 621 Hz values.[35,36] The through-metal ^{31}P−^{31}P trans coupling is clearly influenced by ancillary ligation on

Scheme 4

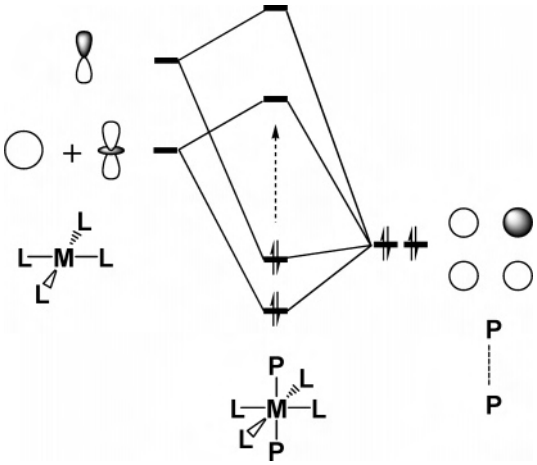

the metal ion. This effect arises from contributions of paramagnetic excited states to the coupling.[51,53] Filled s donor orbitals on two trans phosphorus atoms form symmetric and antisymmetric combinations that interact with the metal-centered gerade s and d_{z^2} orbitals and with the ungerade p_z orbital, respectively (Scheme 4). The supporting equatorial ligand field will also interact with the s and d_{z^2} orbitals but not the p_z orbital. Therefore, the donor properties of the supporting ligands will modulate the energy gap of the $\sigma-\sigma^*$ transition and thus its contribution to the observed coupling. The Fermi contact contribution is presumably much smaller and should mirror the $^1J_{PH}$ trend, as in comparison of neutral *trans*-$[RuCl_2(PH_2Fc)_4]$ and dicationic $[Pd(PH_2Mes)_4]^{2+}$ (Table 3).[32]

There are several compelling motives to extend the initial investigation of primary and secondary phosphine coordination on ruthenium(II) as reported herein. First, the various contributions to the observed $^2J_{PP}$ coupling constants might be quantitatively resolved if the overall paucity of data for complexes of primary and secondary phosphines is ameliorated. Such a development could lead to a straightforward scale of coordinate bonding if the paramagnetic contribution could be calibrated to $\sigma-\sigma^*$ gaps calculated by high-level theory. Furthermore, the synthetic utility of these phosphine complexes as phosphide and phosphinidene ligand precursors has been the subject of only cursory examination.[15]

Acknowledgment. We thank the Ohio University Office of the Vice President for Research for support of the Chemistry and Biochemistry at the Materials Interface Exchange Program with the University of Leipzig. Additional startup support was also received from Ohio University (M.P.J.).

Supporting Information Available: CIF file for *trans*-$[RuCl_2(PH_2CH_2C_5H_4FeC_5H_5)_4]$; empirical exposition on the NMR simulations (5 pages). This material is available free of charge via the Internet at http://pubs.acs.org.

IC0519281

(51) Bertrand, R. D.; Ogilvie, F. B.; Verkade, J. G. *J. Am. Chem. Soc.* **1970**, *92*, 1908−1915.
(52) Ogilvie, F. B.; Jenkins, J. M.; Verkade, J. G. *J. Am. Chem. Soc.* **1970**, *92*, 1916−1923.
(53) Bright, A.; Mann, B. E.; Masters, C.; Shaw, B. L.; Slade, R. M.; Stainbank, R. E. *J. Chem. Soc. A* **1971**, 1826−1831.
(54) Goggin, P. L.; Goodfellow, R. J.; Knight, J. R.; Norton, M. G.; Taylor, B. F. *J. Chem. Soc., Dalton Trans.* **1973**, 2220−2226.
(55) Goodfellow, R. J.; Taylor, B. F. *J. Chem. Soc., Dalton Trans*. **1974**, 1676−1684.
(56) Fontaine, X. L. R.; Kennedy, J. D.; Shaw, B. L.; Vila, J. M. *J. Chem. Soc., Dalton Trans.* **1987**, 2401−2405.
(57) Lubián, R. T.; Paz-Sandoval, M. A. *J. Organomet. Chem*. **1997**, *532*, 17−29.
(58) Keiter, R. L.; Benson, J. W.; Keiter, E. A.; Harris, T. A.; Hayner, M. W.; Mosimann, L. L.; Karch, E. E.; Boecker, C. A.; Olson, D. M.; VanderVeen, J.; Brandt, D. E.; Rheingold, A. L.; Yap, G. P. A. *Organometallics* **1997**, *16*, 2246−2253.